Reliability-Gated Multimodal Evaluation of Finger-Ring Physiological Sensing During Postural and Walking States

Shen Xi, Fei yu and Wu Yuhan*

[1] Shanxi Key Lab for Modernization of TCVM, College of Life Science, Shanxi Agricultural University, Taiyuan 030000, Shanxi, P. R. China
* Correspondence: 387687@163.com

Abstract: The finger-mounted biomedical sensors provide a relatively small form factor for multiple measurements of cardiovascular and autonomic biomarkers on regular occasions. But it is important to know if the obtained biomarkers could be interpreted under conditions of changing optical coupling, contact pressure, and beat detection. In this paper, the analysis of the multimodal platform that allows synchronous recording of electrocardiography, red and infrared photoplethysmography, galvanic skin response, respiratory modulation, and motion was performed. The research question was how summary statistics of the protocol allow distinguishing between reliable stationary discrimination and less reliable ambulatory interpretation. Thus, the reliability-gated analysis was performed for the mean and standard deviation data presented in the paper. Hedges' g was used to rank the standardized separation between the biomarker states, whereas a directional concordance index was calculated in order to determine the consistency of biomarker families under different operating conditions. The contrast of SUPINE to STAND allowed identifying the internally consistent stationary response with the total concordance of cardiac and pulse-arrival-time biomarkers, including large effects for LF/HF$_{PAT}$, CE$_{RR}$, CE$_{PPir}$, LF/HF$_{PPir}$, HR$_{PPir}$, LF/HF$_{RR}$, and HR$_{RR}$. The contrast of SIT to WALK showed a well-maintained gross activation in terms of heart rate, galvanic skin response, and respiration. But the directional consistency of the biomarkers derived from the PPG became very poor (from 100.0% of stationary markers to 42.9% of ambulatory markers).

Keywords: smart ring; finger-worn sensor; photoplethysmography; electrocardiography; galvanic skin response; pulse arrival time; Hedges g; wearable reliability

Citation: Shen Xi, Fei yu and Wu Yuhan. 2025. Reliability-Gated Multimodal Evaluation of Finger-Ring Physiological Sensing During Postural and Walking States. *TK Techforum Journal (ThyssenKrupp Techforum)* 2024(3): 16–27.

Received: June-19-2024
Accepted: December 13-2024
Published: January-30-2025

1. Introduction

Continuous physiological measurement has advanced from specialized laboratory equipment to small wearable technologies that can capture repeated readings outside the lab environment. The significance of this advance is clear since cardiac control, autonomic tone, recovery from sleep, stress response, and activity are dynamical processes that cannot be adequately captured by static readings [1–3]. Wearable technologies present a new scientific challenge in turn: the challenge is not only in capturing physiological signals, but in determining which computed quantities remain physiologically meaningful in the context of motion, temperature variation, inconsistent contact, sweating, peripheral vasoconstriction, and uncontrolled motion [4–6].

Photoplethysmography (PPG) is key to this challenge since it is small, energy-efficient, and compatible with wrist, finger, ear, and ring-based designs. The optical pulse wave can serve as a basis for estimating the heart rate, pulse rate variability, respiratory influence, oxygen saturation, vascular timing, and signal quality [7–9]. However, the same wave is extremely susceptible to pressure, motion, mechanics of the recording site, sensor geometry, and blood flow. The effect of motion artifact can preserve the dominant frequency but distort the wave morphology and interbeat intervals, meaning that heart rate can still remain a useful quantity when the variability indices are distorted beyond recognition [10–

12]. Therefore, PPG-derived biomarkers must be validated on a per-operational-condition basis.

The finger has several distinct advantages for optical and electrical sensing. It is well-perfused, it enables a ring design that can be worn continuously, and it allows the positioning of optical emitters, photodetectors, and contact electrodes in close proximity to the stable vascular bed [13–15]. Several recent validation studies of commercial and research ring sensors have shown that finger PPG provides a reliable base for nocturnal or low-motion heart-rate and heart-rate-variability estimation in comparison with ECG references [16,17]. While this result justifies the ring design as a high-value form factor, it does not demonstrate that all interval-derived or nonlinear variables are valid in walking conditions, where cyclic hand motion and varying tissue pressure can distort the optical path.

Therefore, it is necessary to distinguish between the measurement of the rate level and interpretation at the variability level. The heart-rate variability computed from the ECG signal is well-established marker of autonomic function, which has accepted time-domain, frequency-domain, and nonlinear characteristics [18–20]. The pulse-rate variability computed from the PPG signal may approximate the HRV under favorable circumstances, but agreement becomes fragile when nonstationarity and free-living monitoring are involved [21–23]. Comparative studies under non-lab conditions confirmed this distinction since it was found that the PPG-derived HR and HRV do not deteriorate equally; the former are generally more robust than the latter [24,25]. Therefore, this distinction is crucial for the ring device because it decides whether the technology will be positioned as the broad physiological state monitor or the activity and rate tracker.

The combination of several sensing modalities can enhance the interpretation of the results because the separate channels reflect the different physiological mechanisms. ECG provides the timing information; PPG captures peripheral pulse timing and morphology; galvanic skin response (GSR) indicates sympathetic sudomotor activity; respiration-related modulations provide information about the cardiorespiratory state; and inertial sensing informs about the motion environment [26–28]. The synchronization of these channels in one direction enhances the trust in the physiological interpretation. The divergence of the channels makes the interpretation ambiguous since it may be caused by modality-specific physiology, artifact susceptibility, or poor signal quality for some classes of biomarkers.

In this study, this question is addressed with the help of the published finger-based device that records ECG, red and infrared PPG, GSR, and motion signals in six healthy volunteers in the phases of SUPINE, STAND, SIT, and WALK [29]. The importance of this device is that it is not a single-output consumer ring, but a multimodal research platform. This protocol is also valuable since it includes the low-motion postural transition and the ambulatory transition, which enables testing of the possibility of the separate interpretation of the ring's signals depending on the operational condition.

The research question is clear: given only the mean values and standard deviations of each phase, is it possible to determine which biomarkers remain physiologically consistent in stationary and walking states? The answer to this question cannot be limited to the listing of the numerical differences because the large difference can be physiologically valid in one channel and caused by the artifacts in another. In this case, the analysis has to combine the effect size metric with the index of the directional consistency and the reliability gate. Such approach provides three dimensions of the analysis: the magnitude, physiological direction, and signal-condition consistency. It prevents the discussion from the unjustified emphasis on the walking-state variability results just because they appear to be numerically large.

2. Materials and Methods

2.1. Device data and protocol

The numerical results, device description, protocol parameters, and sample evidence signals employed in this assessment were derived from the published study of the ring-

device conducted by Volpes *et al.* [29]. The study cohort comprised six healthy participants, three females, aged on average 27.3 ± 2.9 years. Each subject performed two sets of paired recordings lasting about 12 min each: SUPINE then STAND, and SIT then treadmill WALK at 4 km/h. The device simultaneously recorded ECG, red and infrared PPG, GSR, motion, and respiration-related signals. The current paper re-employs the phase-wise mean $\pm$ standard deviation numbers and interprets them using the reliability-based statistical perspective.

Figure 1 shows the context of the device in a photograph. The picture is provided solely for visual orientation of the ring form factor. The core analytical issue here is that the compact geometry forces optical, electrical, and electrodermal electrodes to be positioned in a small area of a curved surface, thus requiring the good quality of contact and movement.

Figure 1. Finger-worn sensing ring.

As can be seen from the electronics layout shown in Figure 2, the multi-modality of the platform is quite apparent. The optical and electrical channels measure non-identical features: optical subsystem provides information on the changes in the peripheral blood volume, ECG electrodes provide the cardiac electrical activity timeline, GSR measures the electrodermal conductance, and the inertial module records the movement context. Such diversity of the hardware components justifies the analysis of cross-modal coherence rather than employing one biomarker.

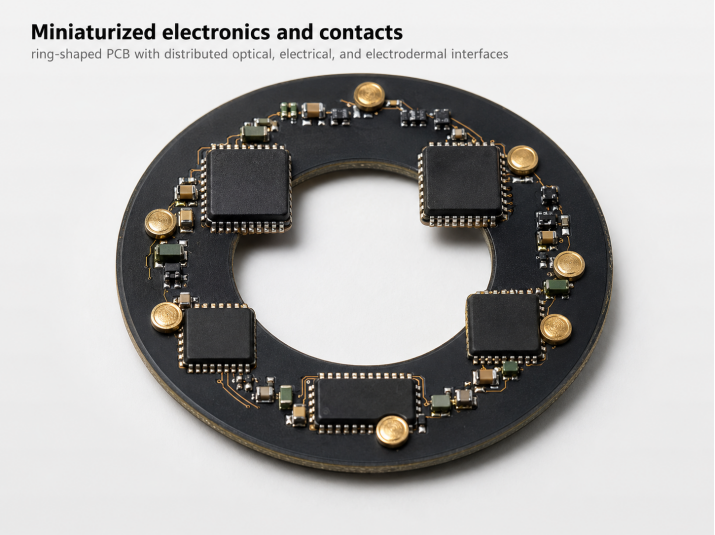

Figure 2. Ring electronics and contacts.

2.2. Effect-size calculation

For each biomarker and protocol contrast, standardized separation was calculated with Hedges g:

$$g = J\frac{\Delta\mu}{s_p}, \tag{1}$$

where $\Delta\mu$ denotes the difference between the phase means written in the expected physiological direction. The correction factor was

$$J = 1 - \frac{3}{4(n_1 + n_2) - 9}, \tag{2}$$

and the pooled standard deviation was

$$s_p = \sqrt{\frac{(n_1 - 1)s_1^2 + (n_2 - 1)s_2^2}{n_1 + n_2 - 2}}. \tag{3}$$

In this data set $n_1 = n_2 = 6$. Formulas (1)-(3) standardize variables to have the same effect size scale. It is necessary due to the diversity of units of the biomarkers: beats per minute, milliseconds, unit-less spectral ratios, entropy, microsiemens, oxygen saturation, and respiratory frequency. Positive g means that the biomarker changes as expected, while negative one shows the lack of concordance between the measured phase shift and the predetermined physiological criterion. It is merely a descriptive calculation, which does not introduce any new inferential model at the individual level.

2.3. Directional concordance and reliability gate

To test whether the biomarker set responded coherently, the directional concordance index (DCI) was defined by the equation

$$\mathrm{DCI} = 100 \times \frac{N_{\mathrm{expected}}}{N_{\mathrm{evaluated}}}. \tag{4}$$

Here, N_{expected} is the number of evaluated markers that changed in the expected direction and $N_{\mathrm{evaluated}}$ is the number of biomarkers involved in the contrast-specific concordance calculation. Eq. (4) is not an equivalent of effect size; rather, it asks an alternative question - whether the multimodal response is internally consistent. A contrast can feature big effects and yet score low on DCI if only a few markers change predictably whereas most others change in the wrong way.

The stationary DCI calculation was limited to the fourteen cardiac, PPG-interval and PAT markers for which the direction rules for the orthostatic contrasts are physiologically direct. GSR, respiration and SpO_2 were kept for descriptive purposes due to possible influence of tonic arousal, respiration pattern and inter-individual differences in measurement precision respectively. In the case of ambulatory contrast, the evaluated set includes HR_{PPir}, $SDNN_{PPir}$, $RMSSD_{PPir}$, LF/HF_{PPir}, CE_{PPir}, GSR and respiration. SpO_2 during walking phase was not included into concordance calculations due to large reported standard deviation compared to the mean change.

The reliability gate was determined from the agreement evidence for ECG-derived and PPG-derived intervals. Stationary and sitting phases represent high-confidence conditions for interpreting the interval information. Walking is a low-confidence condition for optical measures of variability due to potential distortion or amplification of the beat-to-beat intervals caused by the movement even in the absence of mean HR loss.

3. Results and Discussion

3.1. Stationary signals stability and context of their movement

The stationary waveform in Figure 3 displays ECG and PPG (red and IR channels) from the moment of the postural change SUPINE to STAND. The most important here is not visual design but the rhythm stability. ECG complexes and optical pulses are stable enough to provide the interpretation on the basis of intervals, especially before and after the posture change. This visualization confirms the suitability of using stationary signals for the interpretation of cardiac signals, pulse-intervals and PAT.

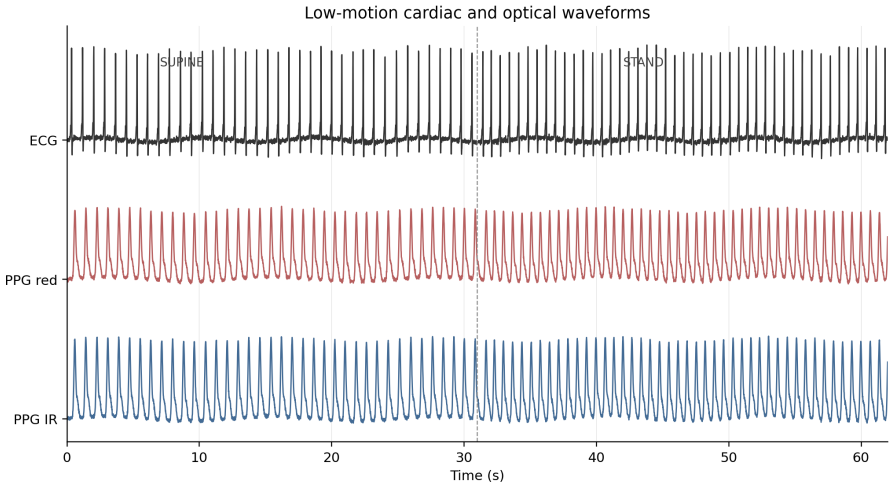

Figure 3. Stationary ECG and PPG waveforms.

Figure 4 displays an additional electrodermal and motion information. While GSR slowly increases after the posture change, acceleration happens mostly at the time of the change itself. This figure confirms the interpretation that the stationary comparison includes the actual physiological reaction but does not put all the signal under influence of locomotor activity. This difference explains the different behaviour of interval-based parameters in the walking phase.

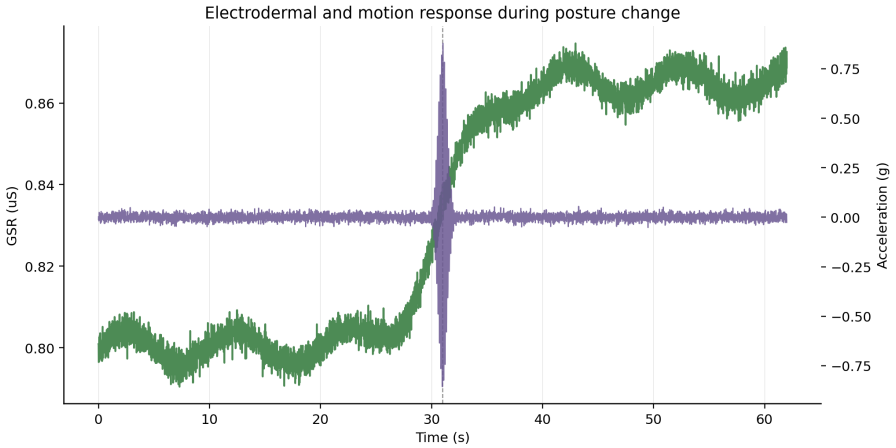

Figure 4. GSR and motion during posture change.

3.2. Interval agreement as the basis of reliability gating

Figure 5 shows the stationary comparison of intervals derived from PPG and ECG; the scatter points are tightly aligned along the identity line, indicating that optical timing can follow electrical timing at rest. The variability measures obtained from the PPG signal may be employed to interpret the SUPINE to STAND transition.

Figure 6 illustrates a more dispersed scatter plot. The same relationship exists between the two intervals but with higher dispersion. This is the reason for applying the reliability gate, while walking records can confirm gross activation, including the activation of the autonomic nervous system by evaluating heart rate, GSR, and respiration.

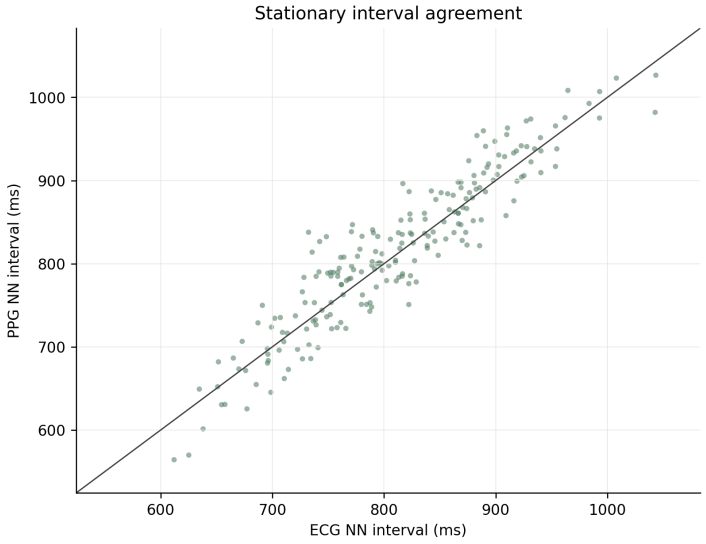

Figure 5. Stationary PPG-ECG interval agreement.

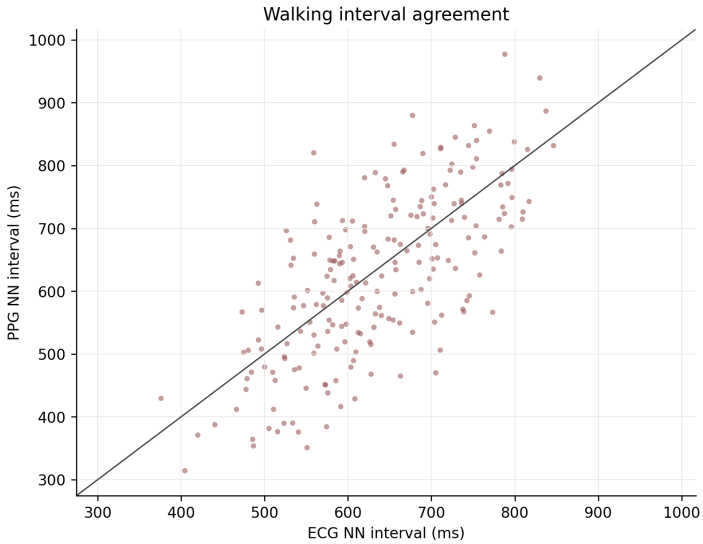

Figure 6. Walking PPG-ECG interval agreement.

3.3. Dataset per Phase

The table below (Table 1) is a repetition of the values obtained at each phase prior to standardization. A number of trends can be observed before standardization. The heart rate shows an increasing trend in both protocols compared. The mean PAT decreases when progressing from the SUPINE to the STAND phases, suggesting that the time of arrival of the peripheral pulse increases with posture change. The GSR increases slightly during STANDING and significantly during WALKING.

Table 1 is important since the study cannot be based only on abstract indices. Data show that the most significant changes during walking do not occur uniformly for all channels. For example, heart rate (HR), galvanic skin response (GSR), and respiration are activated; the variability of the photoplethysmogram (PPG) changes contrary to expectations of reliable optical interval extraction under the influence of motion.

Table 1. Phase-wise values, mean ± standard deviation.

Measure	SUPINE	STAND	SIT	WALK
HR_{PPir} [bpm]	73 ± 12	87 ± 16	77 ± 8	100 ± 10
$SDNN_{PPir}$ [ms]	55.55 ± 20.94	51.10 ± 21.26	58.65 ± 25.05	85.22 ± 42.08
$RMSSD_{PPir}$ [ms]	57.47 ± 37.57	38.46 ± 17.95	47.16 ± 25.19	109.94 ± 72.57
LF/HF_{PPir}	0.68 ± 0.30	2.12 ± 1.94	1.30 ± 0.44	1.17 ± 1.10
CE_{PPir} [nats]	1.20 ± 0.12	0.94 ± 0.31	1.07 ± 0.10	1.27 ± 0.23
HR_{RR} [bpm]	74 ± 12	87 ± 16	77 ± 8	–
$SDNN_{RR}$ [ms]	51.53 ± 20.14	48.68 ± 21.91	59.48 ± 24.96	–
$RMSSD_{RR}$ [ms]	44.55 ± 19.79	31.31 ± 21.63	50.14 ± 26.06	–
LF/HF_{RR}	1.05 ± 0.54	3.41 ± 3.55	1.46 ± 0.93	–
CE_{RR} [nats]	1.13 ± 0.12	0.76 ± 0.34	1.08 ± 0.21	–
Mean PAT [ms]	372.60 ± 51.01	349.92 ± 26.47	396.31 ± 60.71	–
STD PAT [ms]	14.49 ± 9.26	17.25 ± 9.57	19.66 ± 12.38	–
LF/HF_{PAT}	0.39 ± 0.14	1.03 ± 0.44	1.08 ± 0.24	–
CE_{PAT} [nats]	3.92 ± 0.80	4.15 ± 0.51	4.07 ± 0.59	–
GSR [μS]	0.80 ± 0.21	0.86 ± 0.14	1.11 ± 0.39	3.17 ± 1.04
SpO_2 [%]	97.8 ± 1.6	98.7 ± 1.7	99.9 ± 0.19	88.05 ± 21.11
Respiration [Hz]	0.27 ± 0.04	0.23 ± 0.06	0.25 ± 0.07	0.32 ± 0.03

3.4. Standardized biomarker separation

Figure 7 shows the computed Hedges g values. The SUPINE to STAND pattern is concentrated on the positive side for the evaluated cardiac and PAT markers. $\mathrm{LF/HF}_{PAT}$ shows the largest stationary effect ($g = 1.81$), followed by CE_{RR} ($g = 1.34$), CE_{PPir} ($g = 1.02$), $\mathrm{LF/HF}_{PPir}$ ($g = 0.96$), HR_{PPir} ($g = 0.91$), $\mathrm{LF/HF}_{RR}$ ($g = 0.86$), and HR_{RR} ($g = 0.85$). The ring therefore captures orthostatic separation through several mechanisms rather than through heart rate alone.

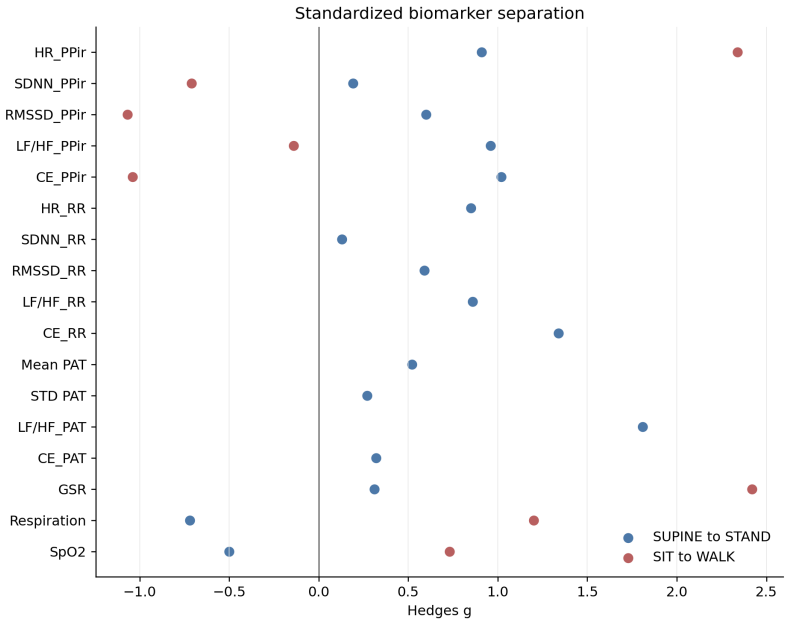

Figure 7. Standardized biomarker effects.

The walking contrast produces a different effect-size geometry. HR_{PPir} ($g = 2.34$), GSR ($g = 2.42$), and respiration ($g = 1.20$) are strongly positive. In contrast, RMSSD_{PPir} ($g = -1.07$), CE_{PPir} ($g = -1.04$), and SDNN_{PPir} ($g = -0.71$) are negative because their walking-state behavior conflicts with the predefined physiological direction. Figure 7 therefore shows the central result of the paper: ambulation does not erase all information, but it narrows the reliable information to rate-level and tonic activation markers.

Table 2 adds numerical precision to the visual result. In the stationary contrast, most cardiac and PAT variables are positive, but the magnitudes differ substantially. SDNN_{RR} and SDNN_{PPir} are close to zero, indicating that broad interval dispersion is not the main orthostatic discriminator. The most informative stationary markers are spectral balance, entropy-related organization, heart rate, and pulse-arrival timing. In the ambulatory contrast, the sign reversal of several optical variability descriptors is not a small numerical artifact; it is the statistical expression of reduced interval reliability during walking.

Table 2. Effect sizes from the reported statistics.

Variable	g (SUPINE→STAND)	g (SIT→WALK)
HR_{PPir}	0.91	2.34
$SDNN_{PPir}$	0.19	-0.71
$RMSSD_{PPir}$	0.60	-1.07
LF/HF_{PPir}	0.96	-0.14
CE_{PPir}	1.02	-1.04
HR_{RR}	0.85	–
$SDNN_{RR}$	0.13	–
$RMSSD_{RR}$	0.59	–
LF/HF_{RR}	0.86	–
CE_{RR}	1.34	–
Mean PAT	0.52	–
STD PAT	0.27	–
LF/HF_{PAT}	1.81	–
CE_{PAT}	0.32	–
GSR	0.31	2.42
Respiration	-0.72	1.20
SpO_2	-0.50	0.73

3.5. Directional coherence

Figure 8 presents the results of the coherence analysis. The stationary marker set showed 100.0% DCI, while the walking marker set showed 42.9% DCI. The discrepancy between these numbers addresses the key analytical question more directly than any effect size. Stationary contrast corresponds to a physiological signature, whereas walking contrast corresponds to a mixed signature in which some channels are useful and other condition-limited.

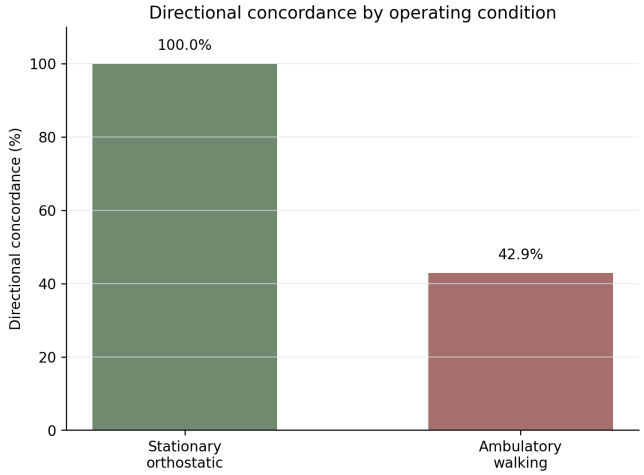

Figure 8. Directional concordance by condition.

Table 3 should be combined with the reading of Figure 8. A DCI score of 100% for the stationary data does not mean that all the variables have equal physiological strength. It means that all selected cardiac and PAT markers behave appropriately. The lower DCI value for the walking data does not mean that the ring fails to function during walking. On the contrary, it means that walking splits the biomarker set into two types: robust activation markers and fragile optical variability markers.

Table 3. Directional concordance index.

Contrast	Markers evaluated	Markers in expected direction	DCI [%]
SUPINE→STAND	14	14	100.0
SIT→WALK	7	3	42.9

The major contribution of this study is a condition-specific interpretation of a finger-worn multimodal sensor. The analysis shows that the same ring cannot be characterized by a universal statement about its validity. The ring's validity depends on the biomarker family and the movement condition. When the condition is SUPINE→STAND, the platform works as a coherent physiological monitor. In SIT→WALK, the platform retains its utility for gross activation but becomes unreliable for variability and entropy analysis of PPG data.

This conclusion is consistent with the current state of wearable technology research. Finger and ring PPG can work very efficiently during periods of low motion, especially for heart rate monitoring during rest and nighttime [15–17]. At the same time, the variability extracted from the PPG waveform is more fragile than heart rate estimation since the latter relies on accurate beat interval detection. In the literature, the comparisons between PPG and ECG data collected under free-living conditions demonstrate the same hierarchical relation: the estimate of the mean heart rate is usually more robust than HRV or PRV descriptors [24,25]. In this dataset, this hierarchy is demonstrated within one protocol based on the ring sensor.

The stationary result is a biophysically plausible conclusion. Orthostatic stimulation induces an increase in sympathetic drive, reduction of vagal tone, increase in heart rate, change in the timing of the vascular phase, and a change in the interval structure. The large value of LF/HF ratio for PAT is consistent with the high sensitivity of pulse arrival timing to the stimulation. The large values of entropy measures, CE_{RR} and CE_{PPir}, suggest that the reorganization of interval structure can be detected reliably in terms of the stationary signals. The agreement between ECG and PPG intervals in the stationary phases confirms that these effects are not optical artifacts.

The walking result should be analyzed differently. Walking increases metabolic demand and autonomic activation; hence, positive effects in HR_{PPir}, GSR, and respiration biomarkers are biophysically reasonable. However, the same movement affects hand dynamics, the pressure at the interface between the sensor and skin, and optical coupling. These effects may introduce an increase and instability of NN interval estimates. Hence, the negative values for $RMSSD_{PPir}$, CE_{PPir}, and $SDNN_{PPir}$ should not be treated as true improvements or expansion of the variability space. These variables are condition-limited optical interval estimates.

For device development, this conclusion implies a clear target of future work. The next target should not be just a stronger PPG signal; the critical target is the validity of NN interval estimation under motion. Better optical positioning, adaptive contact mechanics, beat selection aware of movement, signal quality indexing, and ECG validation should allow preserving the advantages of heart rate estimation and improving the interpretation of the variability. Already, the research-grade adjustable rings and controlled motion validation protocols move in the same direction [30]. This study clearly highlights which endpoint should be used for judging the progress: not only the recovery of heart rate but beat-to-beat PPG interval validity required for variability analysis.

The reliability-gated method also has value beyond this device. In the papers describing new devices, authors typically provide means and standard deviations and not raw waveforms. In such case, additional modeling will introduce false precision. Hedges g and DCI are deliberately moderate tools. They are asking what can be concluded from the provided statistical information without introducing artificial reconstruction of artifact covariance and subject-level details. Such a method is valuable for evaluating prototype devices, peer review, and device comparison when access to the raw data is limited.

4. Conclusions

In this work, the question was addressed of whether the summary statistics provided enough evidence to separate reliably discriminated stationary ring-sensor states from the less reliably discriminated ambulatory interpretations. The answer is affirmative if effect size, consistency, and signal-condition reliability are taken into account. The SUPINE to STAND transition yielded a consistent stationary signature, since the selected heart-rate, PPG-interval, and PAT variables moved in the expected direction, and many of them demonstrated large or very large standardized effect sizes. The SIT to WALK transition yielded a split signature because heart rate, galvanic skin response, and breathing confirmed activation, while the PPG-based variability measures became inconsistent in the presence of motion. Therefore, the ring sensor is a strong tool for stationary autonomic state discrimination and walking-state activation, but not a reliable ambulatory variability analysis tool. Practically speaking, it is now more clear where to draw the line between supported and non-supported activities. It is appropriate to use the ring sensor for guided orthostatic test, seated measurement, recovery evaluation, and ambulatory level monitoring. Walking-state HRV-like variability requires additional interval validation using ECG/PPG waveforms.

Data Availability

The calculations in this manuscript are based on the values reported by Volpes *et al.* [29].

References

[1] Pantelopoulos, A., & Bourbakis, N. G. (2009). A survey on wearable sensor-based systems for health monitoring and prognosis. IEEE Transactions on Systems, Man, and Cybernetics, Part C (Applications and Reviews), 40(1), 1-12.

[2] Patel, S., Park, H., Bonato, P., Chan, L., & Rodgers, M. (2012). A review of wearable sensors and systems with application in rehabilitation. Journal of neuroengineering and rehabilitation, 9(1), 21.

[3] Dias, D., & Paulo Silva Cunha, J. (2018). Wearable health devices—vital sign monitoring, systems and technologies. Sensors, 18(8), 2414.

[4] Bonato, P. (2010). Wearable sensors and systems. IEEE Engineering in Medicine and Biology Magazine, 29(3), 25-36.

[5] Heikenfeld, J., Jajack, A., Rogers, J., Gutruf, P., Tian, L., Pan, T., ... & Wang, J. (2018). Wearable sensors: modalities, challenges, and prospects. Lab on a Chip, 18(2), 217-248.

[6] Smuck, M., Odonkor, C. A., Wilt, J. K., Schmidt, N., & Swiernik, M. A. (2021). The emerging clinical role of wearables: factors for successful implementation in healthcare. NPJ digital medicine, 4(1), 45.

[7] Allen, J. (2007). Photoplethysmography and its application in clinical physiological measurement. Physiological measurement, 28(3), R1-R39.

[8] Shelley, K. H. (2007). Photoplethysmography: beyond the calculation of arterial oxygen saturation and heart rate. Anesthesia & Analgesia, 105(6), S31-S36.

[9] Alian, A. A., & Shelley, K. H. (2014). Photoplethysmography. Best Practice & Research Clinical Anaesthesiology, 28(4), 395-406.

[10] Li, Q., & Clifford, G. D. (2012). Dynamic time warping and machine learning for signal quality assessment of pulsatile signals. Physiological measurement, 33(9), 1491-1501.

[11] Elgendi, M. (2016). Optimal signal quality index for photoplethysmogram signals. Bioengineering, 3(4), 21.

[12] Guo, Z., Ding, C., Hu, X., & Rudin, C. (2021). A supervised machine learning semantic segmentation approach for detecting artifacts in plethysmography signals from wearables. Physiological Measurement, 42(12), 125003.

[13] Asada, H. H., Shaltis, P., Reisner, A., Rhee, S., & Hutchinson, R. C. (2003). Mobile monitoring with wearable photoplethysmographic biosensors. IEEE engineering in medicine and biology magazine, 22(3), 28-40.

[14] Tamura, T., Maeda, Y., Sekine, M., & Yoshida, M. (2014). Wearable photoplethysmographic sensors—past and present. Electronics, 3(2), 282-302.

[15] Kinnunen, H., Rantanen, A., Kenttä, T., & Koskimäki, H. (2020). Feasible assessment of recovery and cardiovascular health: accuracy of nocturnal HR and HRV assessed via ring PPG in comparison to medical grade ECG. Physiological measurement, 41(4), 04NT01.

[16] Cao, R., Azimi, I., Sarhaddi, F., Niela-Vilen, H., Axelin, A., Liljeberg, P., & Rahmani, A. M. (2022). Accuracy assessment of oura ring nocturnal heart rate and heart rate variability in comparison with electrocardiography in time and frequency domains: comprehensive analysis. Journal of Medical Internet Research, 24(1), e27487.

[17] Mastrototaro, J. J., Leabman, M., Shumate, J., & Tompkins, K. L. (2024). Performance of a wearable ring in controlled hypoxia: A prospective observational study. JMIR Formative Research, 8, e54256.

[18] Electrophysiology, T. F. O. T. E. S. O. C. T. N. A. S. O. P. (1996). Heart rate variability: standards of measurement, physiological interpretation, and clinical use. Circulation, 93(5), 1043-1065.

[19] Berntson, G. G., Thomas Bigger Jr, J., Eckberg, D. L., Grossman, P., Kaufmann, P. G., Malik, M., ... & Van Der Molen, M. W. (1997). Heart rate variability: origins, methods, and interpretive caveats. Psychophysiology, 34(6), 623-648.

[20] Shaffer, F., & Ginsberg, J. P. (2017). An overview of heart rate variability metrics and norms. Frontiers in public health, 5, 290215.

[21] Lu, S., Zhao, H., Ju, K., Shin, K., Lee, M., Shelley, K., & Chon, K. H. (2008). Can photoplethysmography variability serve as an alternative approach to obtain heart rate variability information?. Journal of clinical monitoring and computing, 22(1), 23-29.

[22] Gil, E., Orini, M., Bailon, R., Vergara, J. M., Mainardi, L., & Laguna, P. (2010). Photoplethysmography pulse rate variability as a surrogate measurement of heart rate variability during non-stationary conditions. Physiological measurement, 31(9), 1271-1290.

[23] Schäfer, A., & Vagedes, J. (2013). How accurate is pulse rate variability as an estimate of heart rate variability?: A review on studies comparing photoplethysmographic technology with an electrocardiogram. International journal of cardiology, 166(1), 15-29.

[24] Lam, E., Aratia, S., Wang, J., & Tung, J. (2020). Measuring heart rate variability in free-living conditions using consumer-grade photoplethysmography: validation study. JMIR Biomedical Engineering, 5(1), e17355.

[25] Rehman, R. Z. U., Chatterjee, M., Manyakov, N. V., Daans, M., Jackson, A., O'Brisky, A., ... & Morris, M. (2024). Assessment of physiological signals from photoplethysmography sensors compared to an electrocardiogram sensor: a validation study in daily life. Sensors, 24(21), 6826.

[26] Mukkamala, R., Hahn, J. O., Inan, O. T., Mestha, L. K., Kim, C. S., Töreyin, H., & Kyal, S. (2015). Toward ubiquitous blood pressure monitoring via pulse transit time: theory and practice. IEEE transactions on biomedical engineering, 62(8), 1879-1901.

[27] Karlen, W., Raman, S., Ansermino, J. M., & Dumont, G. A. (2013). Multiparameter respiratory rate estimation from the photoplethysmogram. IEEE Transactions on biomedical engineering, 60(7), 1946-1953.

[28] Setz, C., Arnrich, B., Schumm, J., La Marca, R., Tröster, G., & Ehlert, U. (2009). Discriminating stress from cognitive load using a wearable EDA device. IEEE Transactions on information technology in biomedicine, 14(2), 410-417.

[29] Volpes, G., Valenti, S., Genova, G., Barà, C., Parisi, A., Faes, L., ... & Pernice, R. (2024). Wearable ring-shaped biomedical device for physiological monitoring through finger-based acquisition of electrocardiographic, photoplethysmographic, and galvanic skin response signals: Design and preliminary measurements. Biosensors, 14(4), 205.

[30] Montenegro, M., Aliverti, A., & Angelucci, A. (2026). An adjustable smart ring to monitor pulse rate and peripheral blood oxygen saturation. Annals of Biomedical Engineering, 54(3), 885-897.